Evaluation of a set of dispersed phase wall boundary conditions in two-fluid modeling

Mohammed Khalij, Saghir Ba Mohammed Sohail, Oesterlé Benoit

Evaluation of a set of dispersed phase wall boundary conditions in two-fluid modeling

Khalij Mohamed, Saghir Ba Mohammed Sohail, Oesterlé Benoit

LEMTA – Nancy-University, CNRS
ESSTIN, 2 rue Jean Lamour, F-54519 Vandoeuvre-lès-Nancy, France
mohamed.khalij@esstin.uhp-nancy.fr

Keywords: gas-solid, channel flow, wall roughness

Abstract

The effect of wall roughness is known to be particularly important in confined gas-particle flows, as it leads to irregular particle bouncing and significant momentum redistribution in the wall normal direction. In two-fluid or Eulerian models, the particle-wall interactions need to be described by a set of boundary conditions expressing the second and third-order moments of the particle velocities in order to close the transport equations. In this work, the effect of wall roughness is investigated by defining equivalent friction and restitution coefficients, making it possible to extend the formulation of the dispersed phase boundary conditions as established in the smooth wall case. For the model validation, particle statistics at the wall are computed by simulating a large number of particle-wall impacts with a prescribed distribution of the incident velocity. Then, the proposed boundary conditions are evaluated in the case of a particle-laden channel flow through comparison between Eulerian predictions, Lagrangian predictions and available experimental data.

Introduction

One of the approaches that can be used for the numerical simulation of dispersed two-phase flows is the so-called Eulerian-Eulerian approach commonly named "two-fluid model". It is easier to take the presence of the wall into account by Lagrangian simulation, just by using rebound laws and introducing the effect of particle shape or wall roughness by means of a virtual wall model (Tsuji *et al.* 1987, Sommerfeld 1992, Sommerfeld and Huber 1999). In two-fluid models, the wall exists only through the boundary conditions needed for the solution of the differential system. In order to obtain accurate information about the influence of the wall on the behaviour of solid particles, it is important to develop a set of boundary conditions for the dispersed phase. He and Simonin (1993, 1994) and Sakiz and Simonin (1999) established a set of boundary conditions for the dispersed phase at a smooth wall in terms of the Coulomb parameters (coefficients of friction and restitution), using a preassigned binormal PDF for the wall normal particle velocity. Their formalism is based on the determination of the probability density function (PDF) of the particle velocities close to the wall. Using this PDF-two-fluid method, the mean value of any variable at the wall can be expressed as a function of the mean value before collision, and relationships between the various statistical moments of the particle velocity components can be derived, provided that a deterministic rebound law is prescribed. For a rough wall, few studies exist in the case of 2D roughness (Zhang and Zhou 2002, Tanière *et al.* 2004). However, in the work of Zhang and Zhou (2002), the introduction of roughness can result in non zero normal mean velocity, *i.e.* the particle mass flux at the wall is not equal to zero, which is physically incorrect. In the 2D case, Tanière *et al.* (2004) established a set of boundary conditions for the dispersed phase in terms of the equivalent Coulomb parameters (equivalent friction and restitution coefficients), making it possible to extend the formulation of the boundary conditions established in the smooth wall case to a rough wall case. However, as their results were obtained using a pre-assigned incident particle velocity distribution, they are not applicable in a real flow since the actual distribution of the particle velocity in the flow is not taken into account. Simonin *et al.* (2004) suggested a model to describe rough wall boundary conditions but the proposed relations are restricted to elastic impacts, neglecting the so-called shadow effect which was introduced later by Khalij *et al.* (2005).

The aim of this paper is to present a set of wall boundary conditions for the dispersed phase in the 2D roughness case considering inelastic rebounds. The proposed relationships are based on equivalent friction and restitution coefficients, making it possible to use the same formulation of the dispersed phase boundary conditions as established in the smooth wall case. The performance of such boundary conditions is evaluated via an Eulerian-Eulerian simulation of a particle-laden channel flow.

Nomenclature

d_p	particle diameter (m)
e_w	normal restitution coefficient for wall-particle interaction (–)
e_w^*	equivalent restitution coefficient (–)

f	particle velocity distribution function at the wall ($m^{-6}s^3$)
N	number of simulated collisions (–)
n_p	particle number density at the wall (m^{-3})
n_p^-, n_p^+	incident and reflected particle number density at the wall (m^{-3})
$\mathbf{u}$	instantaneous particle velocity vector (m s^{-1})
$\tilde{\mathbf{u}}$	instantaneous reflected particle velocity vector (m s^{-1})
u_x, u_y, u_z	streamwise, wall-normal and spanwise velocity components (m s^{-1})
u_x', u_y', u_z'	fluctuating velocity components (m s^{-1})
$U_{p,i}$	particle mean velocity in direction i (m s^{-1})
U^+, u^+	dimensionless mean and rms fluid velocities in wall units (–)
V^+, v^+	dimensionless mean and rms particle velocities in wall units (–)

Greek letters

g	inclination angle of the virtual wall (–)
s_g	standard deviation of the inclination angle of the virtual wall (–)
m_w	friction coefficient for wall-particle interaction (–)
m_w^*	equivalent friction coefficient (–)

Subscripts

f	fluid
p	particle
x, y, z	direction of vector components in orthogonal system $R(x, y, z)$

Others

$\langle\cdot\rangle$	global statistical average
$\langle\cdot\rangle^-, \langle\cdot\rangle^+$	average on incident and reflected particles, respectively
$\{\bullet\}^-, \{\bullet\}^+$	arithmetic average operators on incident and reflected particles, respectively

Rough wall boundary conditions derivation

Description of the proposed model

Following Sakiz and Simonin (1999), we consider a distribution function *f* for the velocity of the particles at the wall. The mean value of any function y of the velocity is given by:

$$\langle y(\mathbf{u})\rangle = \frac{1}{n_p}\int y(\mathbf{u})\, f(\mathbf{u})\, d\mathbf{u} \tag{1}$$

where $n_p = \int f(\mathbf{u})\, d\mathbf{u}$ is the particle number density at the wall and $\mathbf{u}$ the particle velocity. Thereafter, the components of the velocity vector of a spherical solid particle before and after impact will be denoted by u_i and $\tilde{u}_i$, respectively, in the Cartesian system $R(x, y, z)$ where x, y and z correspond to the streamwise, wall-normal and spanwise directions, respectively. The incident particles have a negative wall normal velocity component, $\mathbf{u}\cdot\mathbf{n} = u_y$, where $\mathbf{n}$ is the unit vector normal to the wall (parallel to the *y* axis), and the reflected particles have a positive velocity component. The fluctuation of y is defined by $y' = y - \langle y \rangle$ and the mean value before and after collision, noted respectively $\langle\cdot\rangle^-$ and $\langle\cdot\rangle^+$, are linked to the mean value $\langle\cdot\rangle$ by the following relation:

$$\langle y \rangle = x\langle y \rangle^- + (1-x)\langle y \rangle^+ \tag{2}$$

where x is defined by $x = n_p^- / n_p$, n_p denoting the number density of the particles moving toward the wall ($n_p = n_p^- + n_p^+$). The reflected wall-normal components of the particle velocity are described by means of the impulsive equations and Coulomb's law, in terms of the restitution coefficient e_w and friction factor m_w. In the case of sliding occurring in the longitudinal direction, and under the condition of negligible spanwise component of the impact velocity for all particles (Sakiz and Simonin 1999), the mechanical rebound laws for the translational velocity components are:

$$\begin{cases} \tilde{u}_x = u_x + m_w\left(1+e_w\right)u_y \\ \tilde{u}_y = -e_w u_y \\ \tilde{u}_z = u_z \ (=0) \end{cases} \tag{3}$$

According to Eq. (2), zero particle mass flux at the wall ($\langle u_y \rangle = 0$) is ensured provided that

$$x = \frac{n_p^-}{n_p} = \frac{\langle \tilde{u}_y \rangle^+}{\langle \tilde{u}_y \rangle^+ - \langle u_y \rangle^-} \tag{4}$$

Using the rebound laws (3), Eq. (4) becomes in the case of smooth wall:

$$x = \frac{e_w}{1+e_w} \tag{5}$$

From Eq. (2), (3), (5), and using an assumption about the distribution of the wall normal incident particle velocity, Sakiz and Simonin (1999) obtained the following boundary conditions at the wall for all computational variables:

$$\begin{cases} \langle u_y \rangle = 0 \\ \langle u_x' u_y' \rangle = -m_w \langle u_y' u_y' \rangle \\ \langle u_x'^2 u_y' \rangle = -2m_w \langle u_x' u_y'^2 \rangle - m_w^2 \langle u_y'^3 \rangle \\ \langle u_y'^3 \rangle = C\dfrac{1-e_w}{\sqrt{e_w}} \langle u_y' u_y' \rangle^{3/2} \end{cases} \tag{6}$$

where *C* depends on the distribution of u_y (for Gaussian distribution, $C = -4/\sqrt{2p}$).

By analogy with Eq. (6), a model is proposed here for the particulate phase boundary conditions in the case of rough wall, based on the equivalent Coulomb coefficients e_w^* and m_w^* defined by :

$$e_w^* = -\frac{\langle \tilde{u}_y \rangle^+}{\langle u_y \rangle^-}, \qquad m_w^* = -\frac{\langle u'_x u'_y \rangle}{\langle u'_y u'_y \rangle} \tag{7}$$

Following Khalij *et al.* (2005), we introduce the parameters l^- and l^+ which characterize the incident and reflected normal velocities distribution, defined by :

$$\langle u_y \rangle^- = -l^- \sqrt{\langle u'_y u'_y \rangle^-}, \quad \langle \tilde{u}_y \rangle^+ = l^+ \sqrt{\langle u'_y u'_y \rangle^+} \tag{8}$$

As the incident normal velocity is negative, l^- and l^+ are positive, and in the case of half-Gaussian distribution of incident velocities we have $l^- = \sqrt{2/p}$. Defining $l = l^- / l^+$, we propose the following relationships to express the 3rd order particle velocity correlations at the wall, by analogy with Eq. (6) :

$$\begin{cases} \langle u'^2_x u'_y \rangle = -2 m_w^* \langle u'_x u'^2_y \rangle - m_w^{*2} \langle u'^3_y \rangle \\ \langle u'^3_y \rangle = C \dfrac{1 - e_w^* l^2}{\sqrt{e_w^*}} \langle u'_y u'_y \rangle^{3/2} \end{cases} \tag{9}$$

Note that for a smooth wall we have $l = 1$ due to the linearity of the rebound law in the wall normal direction. Although the wall is considered as rough, the zero particle mass flux condition at the wall is still ensured ($< u_y >= 0$) since the parameter x is defined by $x = e_w^* / (1 + e_w^*)$ (similar to Eq. (5)). In the rough wall case, we then rewrite Eq. (2) in the following form, where the effects of the restitution coefficient, friction factor and roughness upon the particle phase boundary conditions at the wall are introduced via e_w^* :

$$\langle y \rangle = \frac{e_w^*}{1 + e_w^*} \langle y \rangle^- + \frac{1}{1 + e_w^*} \langle y \rangle^+ \tag{10}$$

In order to close the system, it is necessary to identify e_w^* and m_w^*. The latter coefficient requires knowledge of the wall normal velocity variance $< u'_y u'_y >$ and the kinetic shear stress $< u'_x u'_y >$. In order to evaluate the wall normal velocity variance $< u'_y u'_y >$, we use Eq. (8) so as to obtain :

$$\langle u'_y u'_y \rangle^+ = e_w^{*2} l^2 \langle u'_y u'_y \rangle^- \tag{11}$$

The average of any function y of the velocity is calculated just from an arithmetic averaging method, noted $\{y\}$:

$$\{y\} = \frac{1}{N} \sum_{p=1}^{N} (y)_p \tag{12}$$

with the following relations linking the two averaging operators $\{\bullet\}$ and $\langle \bullet \rangle$:

$$\{y\}^- = \frac{\langle y\, u_y \rangle^-}{\langle u_y \rangle^-}, \quad \{y\}^+ = \frac{\langle y\, u_y \rangle^+}{\langle u_y \rangle^+} \tag{13}$$

The arithmetic mean $\{u'_y\}^+$ of the fluctuating velocity of reflected particles is given by:

$$\{u'_y\}^+ = e_w^* l^2 \{u'_y\}^- \tag{14}$$

From Eqs. (13)-(14), it is possible to obtain the wall normal velocity variance $< u'_y u'_y >$ under the form:

$$\langle u'_y u'_y \rangle^- = \frac{1 + e_w^*}{e_w^* (1 + e_w^* l^2)} \langle u'_y u'_y \rangle \tag{15}$$

which, under the smooth wall assumption (l = 1), reduces to the relation of Sakiz and Simonin (1999), as it should be, *i.e.*:

$$\langle u'_y u'_y \rangle^- = \frac{1}{e_w} \langle u'_y u'_y \rangle$$

The effect of wall roughness can be introduced into Eq. (8) by means of the so-called "virtual wall" model of Sommerfeld (1992). In this model, the actual wall is replaced by a virtual wall, whose inclination angle g (fig.1) obeys a centred Gaussian distribution function with given standard deviation s_g and zero mean value. The generation of only one inclination angle (only one rotation around *z*-axis) traduces the 2D roughness case.

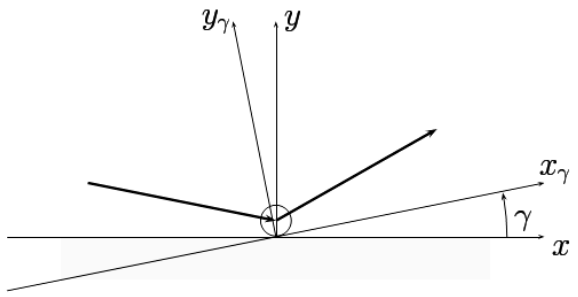

Figure 1: Co-ordinate system and definition of the virtual wall inclination γ.

Attention must be paid to the validity of such rebound laws. Sommerfeld and Zivkovic (1992) showed that the distribution of the inclination angle depends on the impact angle of the particle with respect to the wall (the so-called shadow effect). In order to simulate a physical rebound, some values of the virtual wall inclination angle γ must be avoided. The velocity components in the Cartesian system $R(x, y, z)$ in the case of rough wall are:

$$\tilde{\mathbf{u}}_{|x,y,z} = \mathbf{P}^{-1}\,\mathbf{C}\,\mathbf{P}\,\mathbf{u}_{|x,y,z} \qquad (16)$$

with

$$\mathbf{P} = \begin{bmatrix} \cos\gamma & \sin\gamma & 0 \\ -\sin\gamma & \cos\gamma & 0 \\ 0 & 0 & 1 \end{bmatrix},\quad \mathbf{C} = \begin{bmatrix} 1 & m_w(1+e_w) & 0 \\ 0 & -e_w & 0 \\ 0 & 0 & 1 \end{bmatrix}$$

For small values of virtual wall inclination ($\gamma << 1$), from Eqs.(13), (14) and (16) and by introducing the mean and fluctuating velocity components, $u_x = U_{p,x} + u'_x$, $u_y = u'_y$, e_w^* can be written :

$$e_w^* = \frac{e_w}{l^2} - \frac{(1+e_w)\{\gamma\}^-}{l^2}\left(m_w + \frac{U_{p,x}\langle u'_y\rangle^-}{\langle u'_y u'_y\rangle^-} \right) - \frac{(1+e_w)\{\gamma^2\}^-}{l^2}\left(1 - \frac{m_w U_{p,x}\langle u'_y\rangle^-}{\langle u'_y u'_y\rangle^-} \right) \qquad (17)$$

For $\{\gamma\}^- = 0$ and $\{\gamma^2\}^- = 0$, the restitution coefficient e_w for a smooth wall is retrieved, i.e. $e_w^* = e_w$.

The kinetic shear stress $\langle u'_x u'_y \rangle$ is expressed using Eq. (10) with $y = u_x u_y$:

$$\langle u_x u_y \rangle = \frac{e_w^*}{1+e_w^*}\langle u_x u_y\rangle^- + \frac{1}{1+e_w^*}\langle u_x u_y\rangle^+ \qquad (18)$$

From the relationship (13) that links the arithmetic mean $\{\bullet\}$ and the statistical average $\langle\bullet\rangle$, the following expression of the kinetic shear stress $\langle u'_x u'_y \rangle$ is found :

$$\langle u'_x u'_y\rangle = -\frac{e_w^*}{1+e_w^*}\Big(m_w(1+e_w)\langle u'_y u'_y\rangle^- + \{\gamma\}^-(1+e_w)\left(\langle u'_y u'_y\rangle^- - m_w U_{p,x}\langle u'_y\rangle^-\right) - \{\gamma^2\}^-(1+e_w)\left(m_w\langle u'_y u'_y\rangle^- + U_{p,x}\langle u'_y\rangle^-\right)\Big) \qquad (19)$$

The relationship $\langle u'_x u'_y \rangle = -e_w m_w \langle u'_y u'_y\rangle^-$ derived by Sakiz and Simonin (1999) for a smooth wall is recovered with $\{\gamma^2\}^- = 0$. The approximation proposed by Simonin *et al*. (2004), that is $n_p \langle u'_x u'_y\rangle = 2 n_p^- s_g^2 U_{p,x}\langle u'_y\rangle^-$, is obtained for elastic rebounds (e_w = 1) without friction ($m_w = 0$) and by neglecting the shadow effect ($\{\gamma\}^- = 0$, $\{\gamma^2\}^- = s_g^2$).

Evaluation of the model

The distribution function of the wall-normal velocity of the particles moving toward the wall is noted $f^-(u_y)$, *i.e.* $f^-(u_y)du_y$ is the average number per unit volume of particles with velocity u_y in the range $[u_y, u_y + du_y]$. As the particle number impacting the wall with velocity u_y during time dt is proportional to $|u_y| f_y^-(u_y)dt$, the wall-normal incident particle velocities have to be generated according to a distribution function proportional to $|u_y| f_y^-(u_y)$. In our simulations $f^-(u_y)$ is assumed to be a half-Gaussian distribution. The streamwise component of the particle velocity is assumed to obey a Gaussian distribution with fixed standard deviation.

According to (13) and as suggested by Sakiz and Simonin (1999), the statistical values are computed using the following practical formulas for any function y of the velocity:

$$\langle y\rangle^- = \frac{\sum_{p=1}^N \left(y/|u_y|\right)_p}{\sum_{p=1}^N \left(1/|u_y|\right)_p},\quad \langle y\rangle^+ = \frac{\sum_{p=1}^N \left(\tilde{y}/|\tilde{u}_y|\right)_p}{\sum_{p=1}^N \left(1/|\tilde{u}_y|\right)_p} \qquad (20)$$

The dependence of the equivalent coefficients e^* and m^* upon the roughness parameter s_g in the case of 2D roughness is examined by simulating a large number of particle rebounds (5.10^6). The distribution of the virtual wall inclination angle is Gaussian with given standard deviation s_g and zero mean value. The influence of the virtual wall inclination angle is also studied by testing several values of s_g ranging from 0 to 0.2 according to the results of Sommerfeld and Huber (1999), who showed that the optimum value of s_g decreases with increasing particle diameter for a given physical roughness. As in practical problems the particle fluctuating velocity is generally anisotropic, we set the ratio $\langle u'_x u'_x\rangle^- / \langle u'_y u'_y\rangle^-$ to 2.25. For the tests carried out in this section, calculations are performed assuming a prescribed mean streamwise incident velocity, namely $\langle u_x\rangle^- = 5\sqrt{\langle u'_y u'_y\rangle^-}$.

In order to examine the validity of the model suggested for e_w^*, the results issuing from the numerical simulation are compared with the model in Figs. 2-3, where e_w^* is plotted as a function of the standard deviation s_g for various values of e_w and m_w. It is observed that the proposed model is in almost perfect agreement with the numerical computations. The results can be seen to present some irregular peaks, a behaviour described in Khalij *et al*. (2005), which reflects the possible occurrence of "grazing" rebounds with very small reflected velocity in the wall normal direction. In fact, in some instances the reflected velocity may be very close to zero and consequently the ratio n_p^+ / n_p^- may tend to infinity.

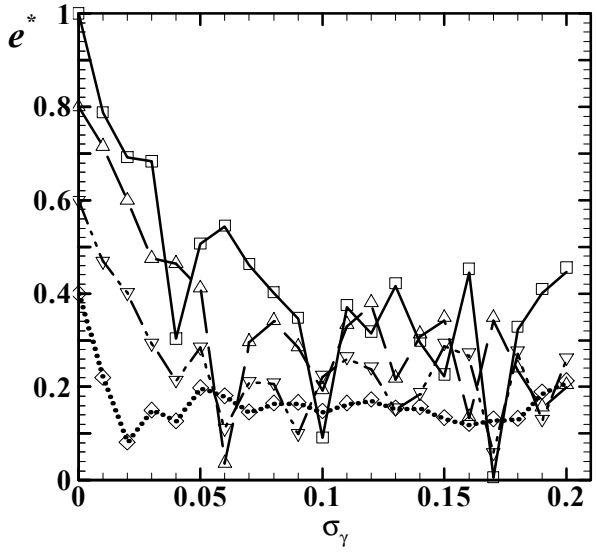

Figure 2: The equivalent restitution coefficient as a function of s_g for $m_w = 0.2$. Comparison between simulation and Eq. (17). Simulations : $e_w = 1$ (□), $e_w = 0.8$ (△), $e_w = 0.6$ (▽), $e_w = 0.4$ (◇). Lines : Eq. (17).

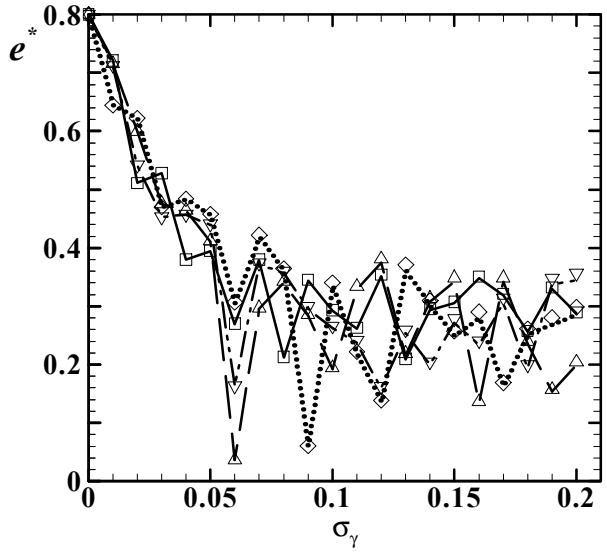

Figure 3: The equivalent restitution coefficient as a function of s_g for $e_w = 0.8$. Comparison between simulation and Eq. (17). Simulations : $m_w = 0$ (□), $m_w = 0.2$ (△), $m_w = 0.3$ (▽), $m_w = 0.4$ (◇). Lines : Eq. (17).

In Fig. 4-5, the validity of the model equation (19) suggested for the kinetic shear stress $< u_x' u_y' >$ is examined. The ratio $< u_x' u_y' > / U_{p,x} < u_y' >^-$ is displayed as a function of the standard deviation s_g for several values of e_w and m_w,

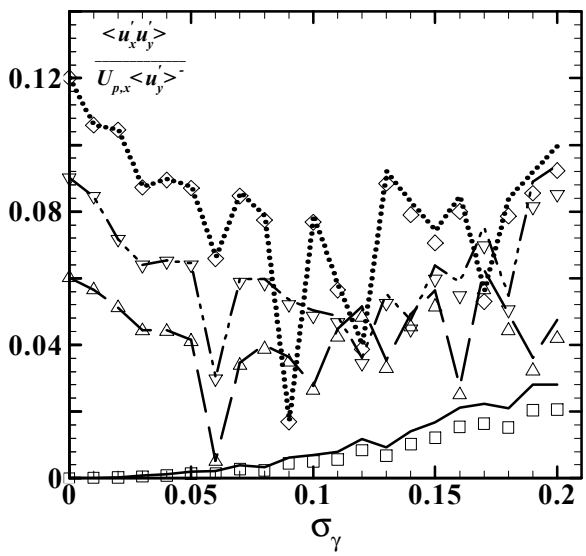

Figure 4: The ratio $< u_x' u_y' > / U_{p,x} < u_y' >^-$ as a function of s_g for $e_w = 0.8$. Comparison between simulation and Eq. (19). Symbols : same caption as Fig. 3. Lines : Eq. (19).

and the results obtained by the simulation are compared with the predictions from Eq. (19). As can be seen, very good agreement between the model and the simulation is obtained for any value of e_w and m_w, even if some slight discrepancies appear when s_g increases. The same remark as above can be made as regards the irregular peaks.

Further comparisons between the model predictions and the numerical simulation are shown in Fig. 6-7 regarding the normalized third-order velocity correlations defined by:

$$\Pi_{yyy} = \frac{\langle u_y' u_y' u_y' \rangle}{\langle u_y' u_y' \rangle^{3/2}}, \qquad (21)$$

shown in Fig. 6, which should be equal to $C(1 - l^2 e_w^*) / \sqrt{e_w^*}$ according to the model equation (9), and

$$\Pi_{xxy} = \langle u_x' u_x' u_y' \rangle, \qquad (22)$$

shown in Fig. 7, which should be equal to $-2m_w^* < u_x' u_y' u_y' > - m_w^{*2} < u_y' u_y' u_y' >$ according to Eq. (9).

As can be seen in Fig 6-7 the obtained values are qualitatively in good agreement with the simulations. The model allows to get satisfactory estimation of Π_{yyy} whatever the value of e_w and m_w. The correlation Π_{xxy} is slightly underestimated by the model for high values of s_g, nevertheless the results are very satisfactory. To summarize, acceptable estimates of the velocity correlations at the wall are obtained by means of a formulation close to the smooth wall formulation of Sakiz and Simonin (1999), using equivalent restitution and friction coefficients.

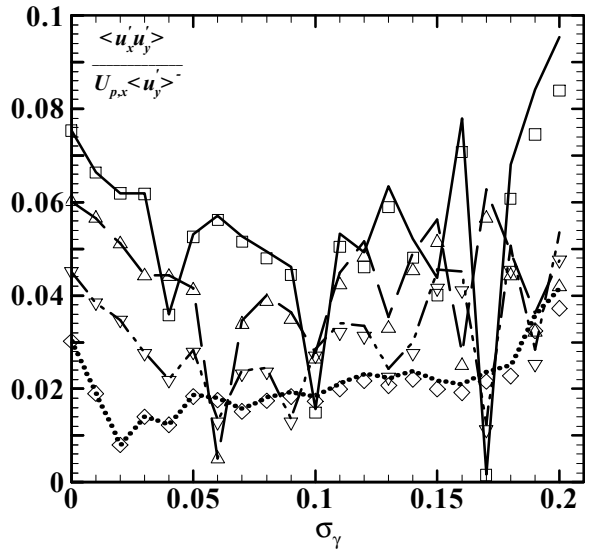

Figure 5: The ratio $< u_x' u_y' > / U_{p,x} < u_y' >$ as a function of s_g for $m_w = 0.2$. Comparison between simulation and Eq. (19). Same caption as Fig. 4.

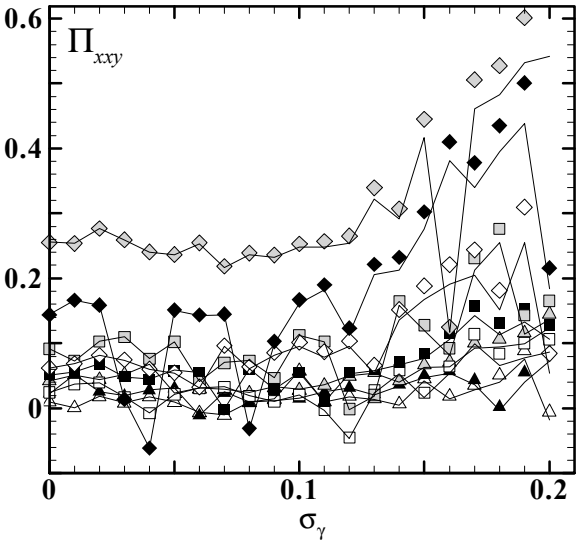

Figure 7: Comparison between the present model and the numerical results for Π_{xxy}. Symbols : same caption as in Fig. 6. Lines : Eq. (22).

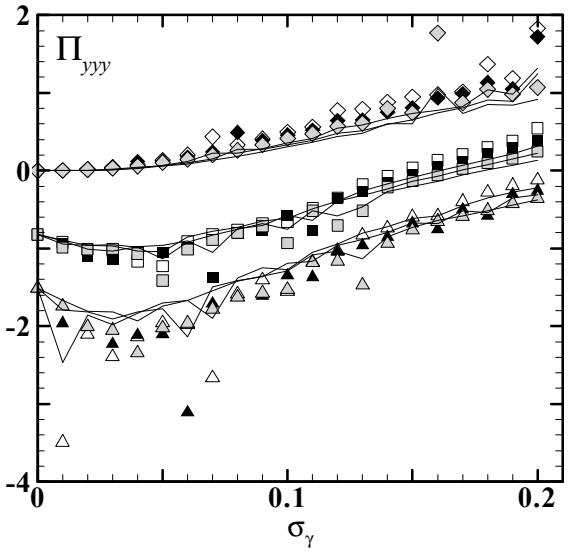

Figure 6: Comparison between the present model and the numerical results for Π_{yyy}. Simulations : $e_w = 0.4$ (△), $e_w = 0.6$ (□), $e_w = 1$ (◇). Empty, black and grey symbols are for $m_w = 0.2$, 0.3 and 0.4., respectively. Lines : Eq. (21).

Numerical simulation of turbulent channel flow, results and discussion

Model description

In this section, the proposed set of boundary conditions is tested by computing a gas-solid turbulent channel flow using an Eulerian-Eulerian model and comparing the results with the Lagrangian simulations carried out by Carlier *et al.* (2005) based on a Langevin stochastic process (SLM), and with the experiments of Khalitov and Longmire (2003) as well. The particle-to-air mass loading in the experiments of Khalitov and Longmire (2003) being of order 10%, the collisions between particles are not considered in this study. For similar reasons, the solid phase can be assumed to be of very low influence on the fluid flow, so that the only coupling effect is the fluid-to-particle one, *i.e.* one-way coupling.

In both the Eulerian and the Lagrangian computations, the data are taken from the experiments of Khalitov and Longmire (2003). Five sets of monodisperse spherical solid particles were tested with mean diameter d_p ranging from $20\ \mu\text{m}$ to $100\ \mu\text{m}$ and density $2500\ \text{kg.m}^{-3}$. The Reynolds number based on the centerline velocity (equal to 10ms^{-1}) and the channel half-width $h = 75\text{mm}$ was $Re_h = 4500$. As pointed out by Lain *et al.* (2002), the standard deviation of the virtual wall inclination depends not only of the wall structure, but also on the particle diameter. Here, we used the values of s_g recommended by these authors for low roughness, namely: $s_g = 0.064$ for $d_p = 20\ \mu\text{m}$, $s_g = 0.061$ for $d_p = 30\ \mu\text{m}$, $s_g = 0.052$ for $d_p = 60\ \mu\text{m}$, and $s_g = 0.043$ for $d_p = 100\ \mu\text{m}$. Further details on the experiment description can be found in Khalitov and Longmire (2003).

The gas flow, considered as incompressible and steady on average, is predicted using a non linear eddy viscosity model (NEVM, Rokni and Sunden 1999), so that turbulence anisotropy is taken into account. In order to provide more precision in the near wall region, modifications of the *k-e* model proposed by Myong and Kasagi (1990) are implemented to account for low Reynolds effects.

For the Eulerian computation of the particle flow, we use the so-called $R_{p,ij} - q_{fp}$ model described by He and Simonin (1993, 1994), which is based on modelled transport

equations for the second-order velocity moments $R_{p,ij} = < u'_{p,i} u'_{p,j} >$ and for the fluid-particle covariance $q_{fp} = < u'_{f,i} u'_{p,j} >$. The boundary condition model described in the previous section is used to account for the roughness effect in particle-wall collisions, with the parameter l^+ as given by Khalij *et al.* (2005), namely $l^+ = 0.4\, l^-$, *i.e.* $l = 2.5$.

The Lagrangian simulation, described in detail in Carlier *et al*. (2005), is performed by tracking a large number of particles, with the fluctuating quantities of the fluid flow at each particle location being predicted by means of a stochastic process based on an extension of the Simple Langevin Model (SLM), using the data provided by the Eulerian calculation. In case of particle-wall collision, the new components of the particle velocity are computed as a function of the velocity components before collision using the complete 3D rebound laws arising from the momentum conservation and Coulomb's law instead of the simplified rebound laws given by Eq. (3). The parameters needed for the processing of collisions are the coefficient of restitution e_w and the coefficients of static and kinetic friction m_w and m_0. The effects of wall roughness are introduced by means of the above described virtual wall model (Sommerfeld 1992), so that direct comparison is made possible between the Eulerian and the Lagrangian computations using the same model for the wall roughness.

In both the two-fluid model and the Lagrangian simulation, the particle-wall collision parameters have been set to the following values: kinetic friction factor $m_w = 0.2$, coefficient of restitution $e_w = 0.95$. The static friction factor needed in the Lagrangian simulation was set to $m_0 = 0.3$, recalling that the boundary condition model for Eulerian computation lies on the assumption of sliding collisions (no need of m_0), whereas the possible occurrence of non sliding collisions is taken into account in the Lagrangian simulation.

Results and discussion

The results presented relate to the case of perfect collisions ($e_w = 1$, $m_w = 0$), the case of inelastic rebound with friction ($e_w = 0.95$, $m_w = 0.2$) and the case of inelastic bouncing with friction on a rough wall. The predictions arising from the Eulerian computation with the above described boundary condition model in these three cases are compared with the numerical results of Carlier *et al.* (2005) obtained through Lagrangian simulation with wall roughness and inelastic frictional collisions ($e_w = 0.95$, $m_w = 0.2$) and the experimental results of Khalitov and Longmire (2003). The dimensionless mean velocities (in wall units) of the fluid, U^+, and of the particles, V^+, are plotted in Fig. 8 as a function of the wall distance y^+ for the various particle diameters investigated. All four plots show relatively good agreement between both the Eulerian and the Lagrangian model and the measured velocities. The gas flow predictions for the mean gas velocity (only shown in Fig. 8(a)) are very satisfactory in the channel core region. Nevertheless, a slight discrepancy for U^+ is noticed very close to the wall, where the Eulerian model for the fluid flow seems to underestimate the experimental data. Despite this difference close to the wall, the mean particle velocity V^+ is well predicted for the three cases studied which seem to differ very slightly in the near wall region. All the numerical results within the whole channel, from wall to centerline, are very close to the experimental data except for the case d_p=100 μm where the experimental results are underestimated by the Eulerian model in the neighbourhood of the wall contrary to the Lagrangian model. For smaller particle sizes, the particle velocity Eulerian predictions with wall roughness seem however to yield better results close to the wall compared to the Lagrangian ones. Among other possible causes, the discrepancies between the two-fluid model with wall

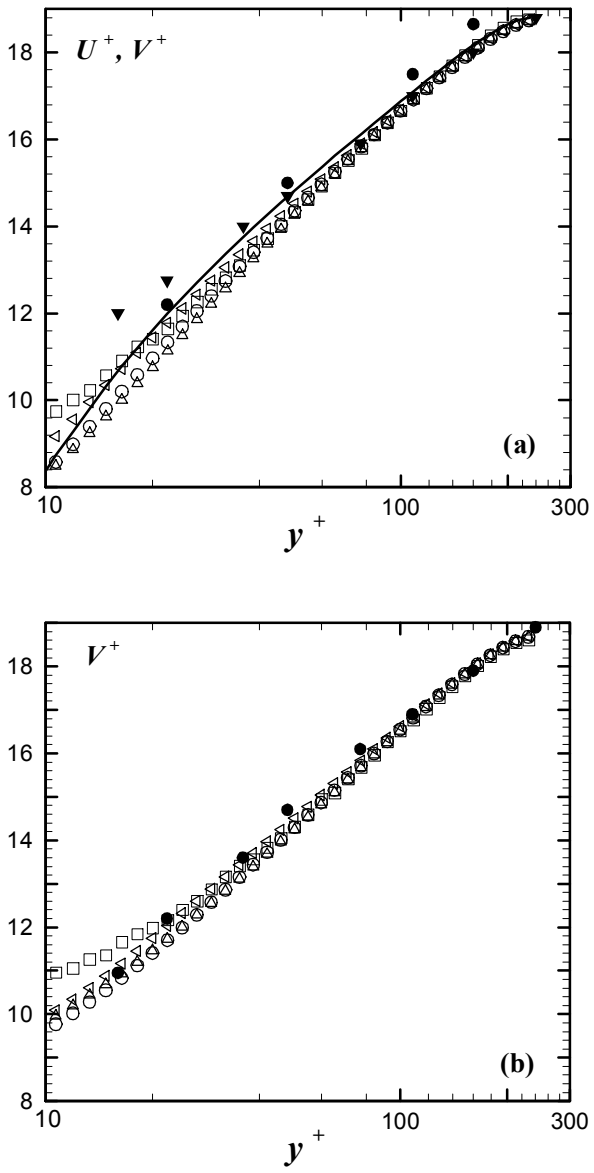

Figure 8(a)-(b): Profiles of dimensionless mean velocities. Experimental data : ▼ unladen gas; ● particles.
Open symbols : Lagrangian simulations (□), Eulerian computations for smooth wall with perfect bouncing (○) or inelastic and frictional bouncing (△) and for rough wall with the present model (◁).
(a) d_p = 20 μm (solid line : predicted gas velocity U^+);
(b) d_p = 30 μm.

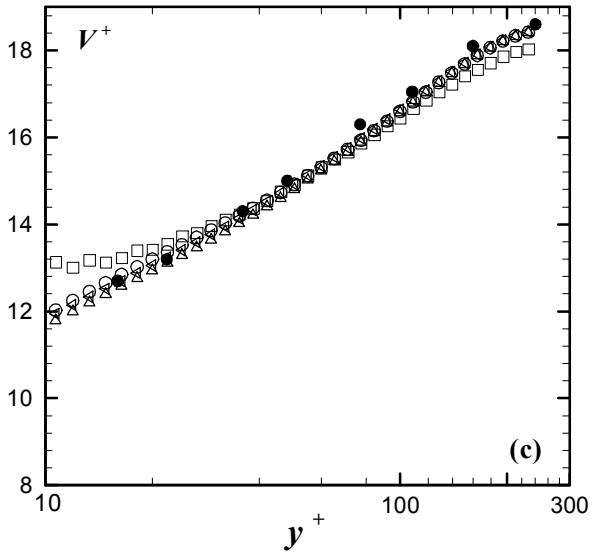

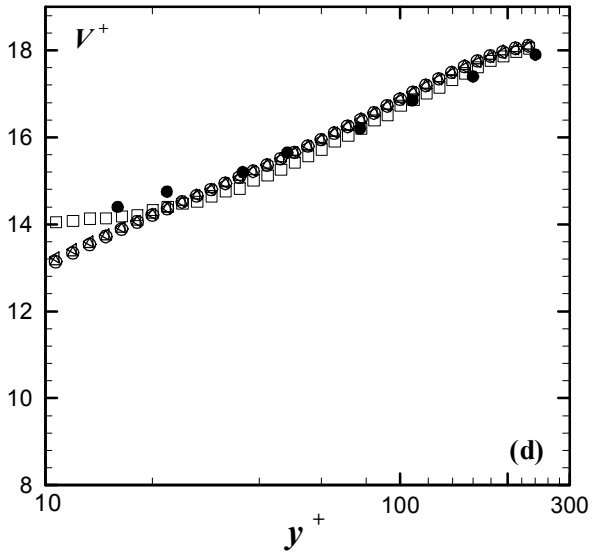

Figure 8 (c)-(d): Profiles of dimensionless mean velocities. Same caption as Fig. 8(a)-(b) except : (c) d_p = 60 µm; (d) d_p = 100 µm.

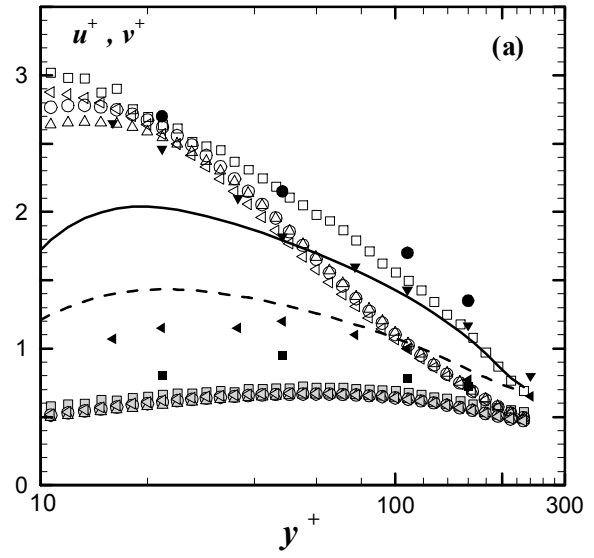

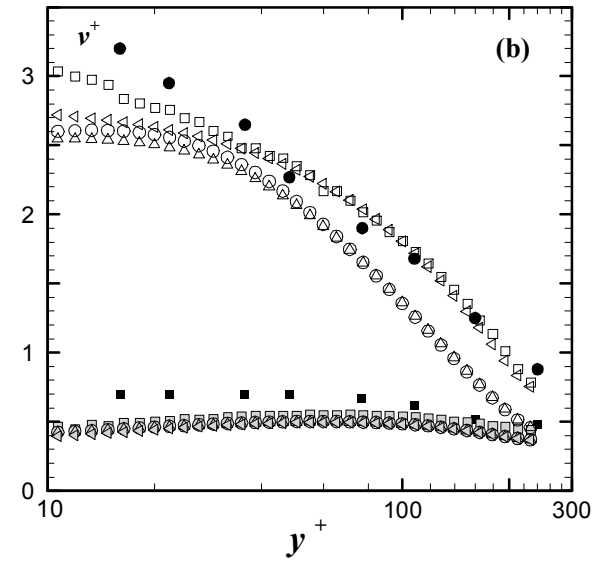

Figure 9(a)-(b): Profiles of dimensionless rms velocities. Experiments : gas: ▼ streamwise, ◄ spanwise; particles: ● streamwise, ■ spanwise. Numerical results for the particle flow : same caption as Fig. 8, with open symbols for the streamwise direction, grey symbols for the spanwise direction.
(a) d_p = 20 µm, numerical results for the gas flow : — streamwise, – – spanwise; (b) d_p = 30 µm.

roughness and the experimental data, in particular for d_p = 100 µm, might be explained by the assumptions that were made to establish the boundary conditions, in particular : half-Gaussian distribution for the incident wall normal velocity of the particles, sliding and nearly two-dimensional collisions, and constant value of the ratio $l^+/l^- = 0.4$ whatever the value of the standard deviation s_g, as suggested by Khalij *et al*. (2005).

Comparisons between the measured and computed profiles of the gas and particle rms velocities (u^+ and v^+, respectively) are presented in Fig. 9. As shown by Fig. 9(a), the predicted rms velocities of the gas are in good agreement with the experimental ones, except in the near wall region ($y^+ < 40$) where the streamwise fluctuating velocity is somewhat underestimated, showing a local maximum at $y^+ \cong 20$ which is not visible in the measurements, whereas the spanwise fluctuating velocity is a little bit overpredicted.

In spite of this small difference between the measurements of Khalitov and Longmire (2003) and the present predictions as regards the gas fluctuating velocity near the wall, the rms velocities of the particles in the streamwise direction are described quite well by the both the Lagrangian and the Eulerian models, as shown by Fig. 9(a)-(d), even if the two-fluid model tends to overestimate the streamwise particle rms velocity for the case d_p = 100 µm. The effect of wall roughness upon the Eulerian

predictions is clearly noticeable by comparing the results obtained with smooth wall (△,○) and with rough wall (◁). The roughness boundary conditions can be seen to lead to improved agreement with the measured values and the result of Carlier *et al*. (2005). The computed values of the spanwise particle velocity fluctuations from the three studied cases as well as for the Lagrangian simulation can be observed to underestimate the experimental results, especially for larger particles. Nevertheless, it can be concluded from Fig. 9 that the numerical predictions with boundary conditions for rough wall in Eulerian-Eulerian predictions appear to be more accurate to estimate the particle fluctuating velocities compared with the results obtained with the assumption that the wall is smooth. The boundary conditions proposed to account for wall roughness seem to appreciably improve the estimate of the particle rms velocities.

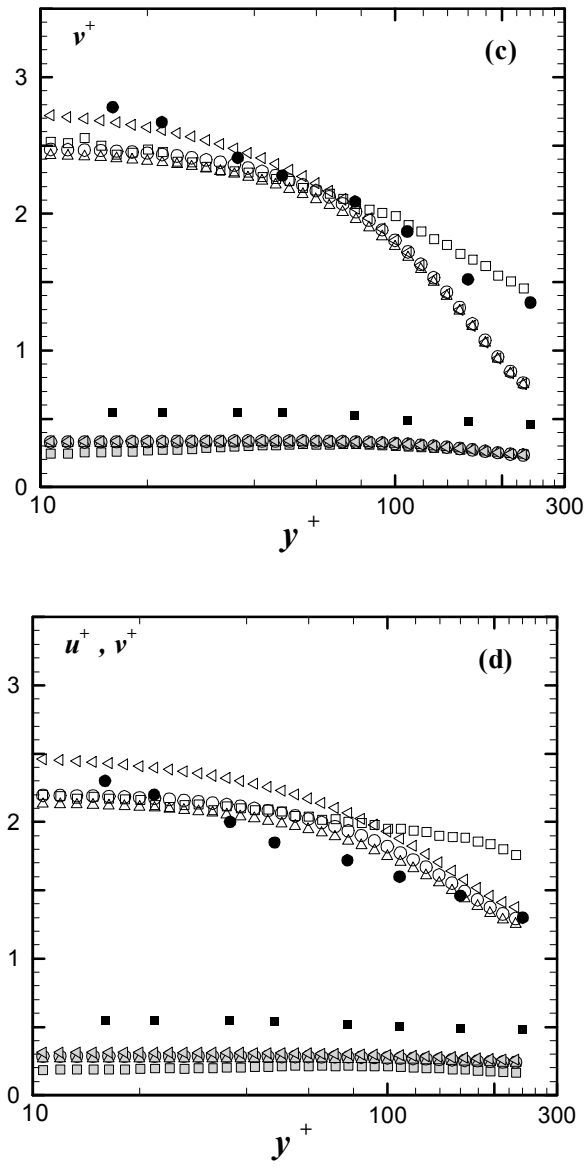

Figure 9(c)-(d): Profiles of dimensionless rms velocities. Same caption as Fig. 9 (a)-(b), except : (c) d_p = 60 µm; (d) d_p = 100 µm.

Conclusions

A boundary condition model for rough walls was proposed to account for irregular bouncing in Eulerian predictions of gas-solid flows. The model is based on equivalent restitution and friction coefficients which can be assessed in terms of the roughness parameter s_g, of the given coefficients e_w and m_w, and of known statistics of the particle motion near the wall, namely $< u'_y u'_y >$ and $U_{p,x}$.

These boundary conditions were implemented in a two-fluid model in order to evaluate their performance in a gas-solid channel flow. The numerical results were compared with the experimental data of Khalitov and Longmire (2003) and with the predictions by the Lagrangian simulation method used in Carlier *et al.* (2005). Good agreement between our results and those of such other works was obtained as regards the particle mean and fluctuating velocities. The numerical predictions are significantly improved when the proposed rough wall boundary condition model is used in the Eulerian computation compared with the case of smooth wall boundary conditions.

References

Carlier, J.-P., Khalij, M. & Oesterlé, B. An improved model for anisotropic dispersion of inertial particles in turbulent shear flows. Aerosol Science and Technology, Vol. 39, 1-10 (2005).

He, J. & Simonin, O. Non-equilibrum predictions of the particle phase stress tensor in vertical pneumatic conveying. In: D. Stock (Ed.), Proc. 5th Int. Symp. on Gas-Solid Flows, ASME Fluids Engineering Division Summer Meeting, Washington D.C., Vol. 166, 253-263 (1993).

He, J. & Simonin, O. Numerical modelling of dilute gas-solid turbulent flows in vertical channel. EDF Report HE-44/94/021/A, Direction des Etudes et Recherches, EDF, France (1994).

Khalij, M., Konan, A., Simonin, O. & Oesterlé, B. On the dispersed phase boundary conditions in gas-solid flows with irregular particle bouncing. In: M. Sommerfeld (Ed.), Proc. 11th Workshop on Two-Phase Flow Predictions, Martin-Luther-Universität Halle-Wittenberg, Merseburg, Germany (CD-ROM, 2005).

Khalitov, D.A. & Longmire, E.K. Effect of particle size on velocity correlations in turbulent channel flow. In: Proc. 4th ASME-JSME Joint Fluids Engineering Conference, Honolulu, Hawaii, paper N° FEDSM03-45730 (2003).

Lain S., Sommerfeld M. & Kussin J. Experimental studies and modelling of four-way coupling in particle-laden horizontal channel flow. Int. J. Heat and Fluid Flow, Vol. 23, 647-656 (2002).

Myong H.K. & Kasagi N. A new approach to the improvement of *k-e* turbulence model for wall-bounded shear flows. JSME Int. J. II, Vol. 33, 63-72 (1990).

Rokni M. & Sunden B. Turbulence modelling experience in duct with forced convection flow. Numer. Heat Transfer A, Vol. 35, 629-654 (1999).

Sakiz M. & Simonin O. Development and validation of continuum particle wall boundary conditions using Lagrangian simulation of a vertical gas-solid channel flow. In: Proc. 3rd ASME/JSME Joint Fluids Eng. Conf., San-Francisco, CA, Paper N° 7898 (1999).

Simonin O., Fede P., Patino G. & Squires K.D., Mathematical models and closure laws for gas-particle turbulent flows. In: Proc. 5th Int. Conf. Multiphase Flows, ICMF'04, Yokohama, Japan, Paper N° K08 (2004).

Sommerfeld M. Modelling of particle/wall collisions in confined gas-particle flows. Int. J. Multiphase Flow, Vol. 18, 905-926 (1992).

Sommerfeld M. & Huber N. Experimental analysis and modelling of particle-wall collisions. Int. J. Multiphase Flow, Vol. 25 1457-1489 (1999).

Sommerfeld M& Zivkovic G. Recent advances in the numerical simulation of pneumatic conveying trough pipe systems. In: Hirsch, Ch., Periaux, J., Onate, E. (Eds.), Computational Methods in Applied Science. Proc. 1st European Computational Fluid Dynamics Conference and 1st Conference on Numerical Methods in Engineering, Brussels, 201-212, (1992).

Tanière A., Khalij M. & Oesterlé B. Focus on the dispersed phase boundary conditions at the wall for irregular particle bouncing. Int. J. Multiphase Flow, Vol. 30, 327-345 (2004).

Tsuji Y., Morikawa Y., Tanaka T., Nakatsukasa N. & Nakatami M. Numerical simulation of gas-solid two phase flow in a two dimensional horizontal channel. Int. J. Multiphase Flow, Vol. 13, 671-684 (1987).

Zhang X. & Zhou L.X. A two-fluid particle-wall collision model accounting for wall roughness. In: M. Sommerfeld (Ed.), Proc. 10th Workshop on Two-Phase Flow Predictions, Merseburg, Germany, 44-51 (2002).